The uneven nature of daily precipitation and its change

Angeline G. Pendergrass[1*] and Reto Knutti[2]

[1]National Center for Atmospheric Research, Boulder, Colorado, USA

[2]Institute for Atmospheric and Climate Science, ETH-Zurich, Zurich, Switzerland

Corresponding author: Angeline Pendergrass (apgrass@ucar.edu)

* The National Center for Atmospheric Research is sponsored by the National Science Foundation.

Key Points:

- Precipitation falls unevenly in time: in the median of observing stations, half of annual precipitation falls in the wettest 12 days.
- In response to warming, unevenness increases in 97% of climate models.
- The increase in precipitation in response to warming occurs primarily during events often considered extreme.

Abstract

A few days with heavy rain contribute disproportionately to total precipitation, while many days with light drizzle contribute much less. What is not appreciated is just how asymmetric this distribution is in time, and the even more asymmetric nature of trends due to climate change. We diagnose the temporal asymmetry in models and observations. Half of annual precipitation falls in the wettest 12 days each year in the median across observing stations worldwide. Climate models project changes in precipitation that are more uneven than present-day precipitation. In a scenario with high greenhouse-gas emissions, one-fifth of the projected increase in rain falls in the wettest two days of the year, and seventy percent in the wettest two weeks. Adjusting modeled unevenness to match present-day unevenness at stations, half of precipitation increase occurs in the wettest 6 days each year.

Plain Language Summary

Rain falls unevenly in time, which can lead to floods and droughts. It is widely known that precipitation is uneven, but it is difficult to quantify. Here we develop a measure for the unevenness of precipitation: the number of the wettest days each year in which half of the annual rain falls. We apply this to rain observed by gauges around the world. At all gauges combined, it takes only 12 days each year for half of the rain to fall. We also apply the measure to climate model simulations, with projections for the rest of the century. In the climate model simulations, the change in future rainfall is even more uneven than rainfall today: in a scenario with high greenhouse-gas emissions, half of the increase in rainfall happens in the wettest 6 days each year. Rather than assuming more rain in general, society needs to take measures to deal with little change most of the time, and a handful of events with much more rain.

1 Introduction

Precipitation falls unevenly in time. Many days have no precipitation, some have steady light rain or snow, and a few have torrential downpours. This unevenness or asymmetry has impacts: stretches with little precipitation can lead to drought, while torrential downpours can lead to floods. Uneven precipitation can affect food security; for example, more unevenness is associated with lower yields of major crops (Fishman, 2016) and grazing land that supports fewer livestock (Sloat et al., 2018). Changes in the unevenness of precipitation would be felt through these impacts. While the unevenness of precipitation and its change with warming are known, they are seldom quantified.

Some work has focused on changes in the unevenness of precipitation. The fraction of total precipitation contributed by extreme events, defined by the 95th percentile of precipitating days, increased during the 20th century (Karl and Knight, 1998; Semenov and Bengtsson, 2002; Groisman et al., 2005). The Gini coefficient originated as a measure of economic inequality and has also been applied to precipitation. By this measure, unevenness of precipitation also increased during the late 20th century (Rajah et al., 2014), and this increase is attributable to anthropogenic emissions (Konapala et al., 2017). But these metrics for the unevenness of precipitation have not been taken up widely. To be useful in research and applications, an ideal metric would be quantitative; to be understood by a broad audience, it would be intuitive. Such a measure has been elusive.

Rather than focusing on its unevenness, more work has examined two aspects of precipitation change separately: its mean and its extremes. In response to warming, it is expected that global-mean precipitation will modestly increase (by ~2 %K^{-1}) while extreme precipitation will increase faster (by ~6 %K^{-1} or more, depending on the definition of "extreme"; e.g., Collins et al., 2013). There are separate explanations for the changes in mean and extreme precipitation. Mean precipitation increase is limited by its role in the planet's energy budget (e.g., Mitchell et al., 1987); it responds to different climate forcing agents according to how they influence the surface and atmosphere. Meanwhile, extreme precipitation change is driven by increasing moisture (e.g., Trenberth, 1999) accompanied by circulation associated with extreme events that varies regionally (e.g., Pfahl et al., 2017) but changes little on average (e.g., Allen and Ingram, 2002).

We have alluded to the variety of ways to define extreme precipitation (see e.g., Seneviratne et al., 2012). Common definitions include the 99th and 95th all-day or wet-day percentile (the 90th percentile is occasionally encountered), another is the wettest day per year. When using less-extreme definitions like the 90th or 95th percentile to diagnose changes in response to warming, the magnitude of increase in response to warming is smaller than with more extreme definitions (Pendergrass, 2018), responding more like mean precipitation than extremes. Given this variation in behavior, it is not clear that the strict separation of precipitation into its mean and extremes is meaningful.

Taken together, the projected changes in mean and extreme precipitation imply an increase in unevenness of precipitation, but they do not provide a path to quantify it. How should we quantify the unevenness of precipitation and its change? To answer this question, we examine the distribution of precipitation, propose a metric that distills the answer, and apply it to observations and model simulations. Furthermore, how much total precipitation is contributed by extreme events? Our analysis of the distribution is readily translated to common definitions of extreme precipitation. We argue that this provides a useful measure of the unevenness of precipitation and its change, and also informs our understanding of extreme precipitation.

2 Data and Methods

We analyze three daily precipitation datasets, quantifying the unevenness of precipitation in two ways.

2.1 Station observations

Station observations provide our best estimate of present-day precipitation at individual locations. We use the Global Historical Climatology Network Daily (Menne et al., 2012a) station observations. We choose stations from the Global Climate Observing System Surface Network, which have higher quality than the full dataset and are distributed globally, though concentrated in North America, Eurasia, and Australia. We include only stations with sufficient temporal coverage: at least 70% of data available for at least 70% of years. For seasonal calculations, we combine each December with the following January and February, and we require data to be present for 70% of days during the season (June, July and August - JJA, and December, January and February - DJF). To translate DJF and JJA into summer and winter seasons, we consider winter to be in DJF the northern hemisphere and JJA in the southern hemisphere (vice versa for summer). As a measure of uncertainty, we use the 25th and 75th quantiles across stations. For comparison with gridded observations, we analyze the period 1999-2014 and include only stations equatorward of 50° latitude, of which there are 185 that meet the inclusion criteria.

2.2 Model simulations

Climate model simulations tell us how the unevenness of precipitation might change in the future. We analyze fully coupled simulations contributed to CMIP5 (Taylor et al., 2012), forced with historical estimates of emissions through 2005, and the Representative Concentration Pathway 8.5 (RCP8.5) and RCP2.6 emissions scenarios from 2006 through 2100 (Meinshausen et al., 2011). We use only the r1i1p1 ensemble member from each model, and only those with daily precipitation data available in the archive (36 models for RCP8.5 and 23 for RCP2.6, listed in Table S1). We use each model's land mask for land-aggregate calculations. We make most calculations on each model's native grid; though for comparison against gridded observations, we regrid the model precipitation to 2.5° resolution. We use a conservative regridding scheme; 2.5° is coarser than 80% of the models. We focus on the period of gridded observations, 1999-2014, for the present, and 2085-2100 (the last 16 years before 2100) for the future. For the present period, we splice historical and RCP8.5 simulations (more simulations are available for RCP8.5 than for other scenarios). For comparison against stations, we choose the nearest gridpoint to each station. For the future period, we analyze the high RCP8.5 emissions scenario as well as the lower RCP2.6 emissions scenario.

2.3 Gridded observations

While station observations measure what is essentially a point, model grid cells represent a larger area (Chen and Knutson, 2008). To bridge the two, we use a gridded observational product, the TRMM 3b42 Multisatellite Precipitation Analysis (Huffman et al., 2007). The TRMM 3b42 data are derived from a combination of station and satellite observations, and are available for the full years 1999-2014, when the TRMM satellite was in orbit, with coverage equatorward of 50° latitude. We aggregate the data to daily frequency. We compare the native 0.25° resolution data with station observations and coarsen this same data to 2.5° with a conservative scheme to compare against model simulations. We analyze the gridpoint closest to each station.

2.4 Fraction of total precipitation by wettest days each year

The first method quantifies unevenness of precipitation as the fraction of total precipitation contributed cumulatively over the wettest days each year. This measure answers the question, "What fraction of the total precipitation falls on the wettest N days of the year?", with N being any number of interest. The goal of this measure is to be intuitive and relatable. It is calculated as follows. First, we take the timeseries of precipitation for each year or season and sort it from high to low daily accumulation, normalized by the total precipitation for that year (for both annual and seasonal analysis). Then, for each year, the cumulative sum of this fraction is calculated, as a function of the number of wettest days in the year. Next, the median of this cumulative sum is calculated across years. Separately, the number of days that constitute half of total precipitation is calculated by interpolating the cumulative fraction each year, and then taking the median across years. Finally, we take the median across stations or gridpoints to calculate area-aggregated values.

2.5 Rain amount survival fraction by percentile

The second method for quantifying unevenness is the fraction of total precipitation as a function of percentile of the cumulative frequency distribution. It answers the question "what fraction of total precipitation occurs beyond the top *p* percentile of days in a period?," where *p* is any percentile of interest. This measure is relevant because these percentiles form the basis for many definitions of extreme precipitation. The main differences from the first method are that the former is expressed as number of wettest days and based on the median of calendar years, while the latter is expressed in terms of percentile-based definitions and is calculated over all days in a period (in our case, each period is 16 years). The measure is calculated counting down from the most extreme precipitation, so we refer to it as the survival fraction. The procedure is as follows: we calculate the all-day frequency distribution of precipitation for the period, and take the sum of the fraction of total precipitation contributed beyond each percentile at each gridpoint or station. For station data, we additionally calculate the wet-day frequency distribution using thresholds of 0 and 1 mm d^{-1}, for comparison with ETCCDI-like indices (Zhang et al., 2011). For summary values, we interpolate to find the percentile beyond which half of precipitation falls, and to aggregate spatially, we take the median across stations or gridpoints.

2.6 Unevenness of precipitation change

Quantifying the unevenness of precipitation change requires further specific considerations. The unevenness of the precipitation change in response to warming is more ambiguous than the unevenness during one period. One ambiguity is that precipitation often increases but sometimes decreases, and its change may even be zero. Where precipitation change is near zero, the fraction of change could is poorly defined. To avoid this, we diagnose the unevenness of precipitation only for spatial aggregated regions where total precipitation increases in response to climate change. This works for many regions, including land, the entire globe, and the tropics and extra-tropics, because precipitation increases in more places than it decreases.

Another ambiguity is that precipitation change is not uniformly positive at all intensities. In response to warming, more precipitation falls on the wettest days; meanwhile, there are fewer days with moderate precipitation (e.g., Pendergrass and Hartmann, 2014a). Because precipitation change is negative for some intensities, the cumulative fraction of precipitation change reaches values greater than one, though it starts at zero and ends at one. The spatially-aggregated cumulative fraction of precipitation change is always positive, though it need not be.

2.7 Change in unevenness at stations

We build on the previous analyses to estimate the number of days during which half of the change is projected to occur at stations. Future projections come from models, which we adjust for biases in present-day unevenness relative to observations (see Section 3). We start from the number of days for half of precipitation at stations at present. Then, we estimate the number of days for half of future precipitation at stations by multiplying the present-day value at stations by the ratio of the multi-model median future to present values. Next, to adjust for the difference between models and stations, we assume that the cumulative fraction of precipitation per day follows an exponential function with a decay parameter determined by the number of days for half of precipitation. We multiply these assumed distributions by the modeled present and future total precipitation, from which we generate the cumulative fraction of precipitation change at stations. Finally, we calculate the number of days for half of this change.

3 Results

The unevenness of precipitation at stations, quantified by the cumulative fraction on the wettest days each year and the contribution beyond percentiles of the distribution, is shown in Fig. 1a,b (black line); selected values are listed in Table 1. A large fraction of precipitation falls in a small number of days – three-quarters of precipitation falls on the wettest 30 days each year, over 1/8 falls on the wettest 2 days, and 1/12 on the wettest day. As a summary metric, we use the number of days each year during which half of annual precipitation falls. For station observations, half of total precipitation falls on the wettest 12 days each year.

The unevenness of precipitation varies with location and season. Figure 2a shows a map of the number of days for half of precipitation. In general, locations that are generally considered dry (in terms of precipitation amount and frequency), like the southwestern US and Australia, have most of their precipitation on a smaller number of days. This contrasts with places that are generally considered wet, including the northeastern US, much of Europe, and the tropical western Pacific. China and southern Russia have half their precipitation in about the median number of days. In locations with strong seasonality, the contribution of the heaviest day each season to annual precipitation also varies seasonally (Fig. 2b,c). A larger fraction of annual precipitation falls on the wettest summer day, 5.2% than on the wettest winter day, 3.4% (equatorward of 50° latitude).

The survival fraction of precipitation as a function of percentile (Fig. 1b) provides context for the unevenness of precipitation in terms of its frequency distribution. More than 3/4 of precipitation falls beyond the 90th percentile, nearly 2/3 falls beyond the 95th percentile, and ~1/4 falls beyond the 99th percentile. To summarize the survival fraction of precipitation by percentile, we focus on two metrics: the percentile beyond which half of precipitation falls, which is 97.0 in the median across stations, and the fraction of precipitation falling beyond the all-day 95th percentile, which is 64% in the median (Table 1). The variations in space of the summary metrics are shown in Fig. 2d,e. The percentile beyond which half of precipitation falls is higher than the 95th at most stations. At some stations, it is even beyond the 99th (Fig. 2d). Correspondingly, most stations have more than half of precipitation beyond the 95th percentile, some over 90% (Fig. 2e). A minority of stations have less than half of precipitation falling beyond the 95th percentile; in these locations precipitation is frequent, like the tropical western Pacific.

We focus on all-day percentiles, but sometimes wet-day percentiles are used to define extreme precipitation instead (Schär et al., 2016). When all days with non-zero precipitation are included in the wet-day count, over 1/3 of precipitation falls beyond the 95th wet-day percentile (Table 1). When only days with at least 1 mm of precipitation are included, ~1/4 of precipitation falls beyond the 95th percentile. These fractions are smaller than for all-day percentiles, but nonetheless substantial.

In climate model simulations, all metrics show that precipitation is less uneven than observed at stations (Fig. 1 orange lines, Table 1). Half of modeled precipitation falls on the wettest 23 days each year, nearly a factor of two more than the stations despite subsampling to match locations. While it is established that models rain too often, primarily in the form of drizzle (Stephens et al., 2010), our metrics focus on heavy rather than light precipitation. Light precipitation contributes little to the total (Pendergrass and Hartmann, 2014b), and counting down from the wettest days and percentiles leaves the drizzle for last. Nonetheless, directly comparing models and station observations is inconsistent because stations measure precipitation at a point in space while model grid cells represent a larger area. To form a bridge, we use gridded observations from TRMM. It is straightforward to coarsen gridded data. We analyze two resolutions: the native 0.25° and coarsened 2.5° (Fig. 1). At its native resolution, the unevenness of TRMM precipitation is consistent with station observations. In the coarsened TRMM data, unevenness decreases by all measures, but remains more uneven than climate model precipitation at 2.5°. The difference in unevenness between stations and models is thus mostly, but not completely, accounted for by the difference in their resolution.

While observations tell us about present-day precipitation, climate models enable us to quantify the unevenness of projected future precipitation and its change from the present. Simulated future precipitation is slightly more uneven than simulated present-day precipitation, though the difference is small (Fig. 1c, Table 1). In the median over land, half of precipitation falls on the wettest 26 days each year at present, and the wettest 25 days at the end of this century.

The change in precipitation, however, is much more uneven than present-day precipitation. Over land, half of the increase occurs on the wettest 8.6 days each year, and beyond the 98.2 percentile (Table 1). The increase in unevenness of the change relative to present is robust across models: of the 36 models analyzed here, 35 have an increase in unevenness by both metrics, while just one has a very slight decrease (Table S2). The wettest day each year (calculated separately for present and future climate states) contributes 12% of the annual mean precipitation change, while over 80% falls beyond the 95th percentile (Table 1). Summary metrics for regions other than global land are listed in Table S2: the whole globe, ocean, tropics, extratropics, and extra-tropical land. Among these, the tropics have the most uneven change in precipitation, half of which occurs during the wettest 7.0 days. Extratropical land has the least uneven precipitation of these regions, but even there, half of precipitation change falls beyond the 95th all-day percentile. For the low emissions scenario RCP2.6, with less warming compared to RCP8.5, the change in precipitation is not as uneven as the high emissions scenario but remains more uneven than present. This indicates that avoiding warming also avoids some of the increase in unevenness of precipitation. We expect unevenness to be even greater at station level, due in part to the difference in resolution shown above. We estimate that at station level half of precipitation change would occur in the 6 wettest days each year.

4 Discussion

We have introduced simple metrics to characterize the temporal unevenness of precipitation. The number of wettest days during which half of precipitation falls tells us how uneven precipitation is at present, and enables us to compare unevenness among locations and datasets. The percentile beyond which half of precipitation falls informs the degree of extreme precipitation that constitutes a majority of total precipitation. The 95th percentile, which is sometimes used as a metric for extreme precipitation, encompasses a majority of precipitation at most observing stations.

Climate models capture much of the observed unevenness of precipitation when their resolution is accounted for. The simulated change in precipitation in response to warming is much more uneven than present-day precipitation. To our knowledge, this is the first study to quantify the unevenness of precipitation change. Our results show that a majority of precipitation change falls in a small number of events that are often considered extreme.

The current narrative is that extreme precipitation change is driven by increasing moisture (with regional modulation by circulation change), while mean precipitation change is muted in comparison because of its role in the planetary energy budget. Our results show that mean and extreme precipitation change have substantial overlap. Essentially all of the increase in precipitation occurs beyond the 90th all-day percentile, over four-fifths occurs beyond the 95th percentile, and nearly 40% occurs beyond the 99th percentile. One implication is that precipitation included in less-extreme definitions of extreme is constrained energetically. This is consistent with the dependence of extreme precipitation change on its definition (e.g., Pendergrass, 2018). In order to simultaneously invoke explanations of precipitation change based on the energy budget and increasing moisture, the definition of extreme precipitation should be very extreme, perhaps the 99.9th all-day percentile or the wettest day each year.

On the other hand, since total precipitation falls disproportionately on just a few days, the monthly or seasonal mean precipitation disproportionately reflects conditions on these days. Monthly or seasonal averages are often used to diagnose the circulation associated with precipitation. Rather than the time mean, focusing only on the circulation when precipitation falls can provide a different perspective. Such an event-based perspective led to new insight on regional interactions between precipitation and circulation (O'Neill et al., 2017).

Previous studies have examined related metrics for the unevenness of precipitation. Sun et al., (2006) calculated the number of days contributing two-thirds of precipitation in models and observations. Their focus was on the spatial pattern of precipitation; they did not report summary statistics from their analysis. They also examined how precipitation frequency varies across broad classes of precipitation intensity. This contrasts with our approach, which focuses on the whole distribution of precipitation (Fig. 1) and its distillation into quantitative metrics (Table 1).

One could ask how this picture would differ for higher temporal frequencies. We analyze daily data because it is widely available; had we used hourly data instead, we expect that the degree of unevenness would be as large or larger (Trenberth et al., 2017).

Another aspect of precipitation that is important for impacts is the sequencing of events in time. For example, if a non-irrigated pasture gets only two days of heavy precipitation just after the end of its ideal period of growth, the grass may fail. If instead these two days of precipitation come at the beginning of the growing season, the season might be successful. Our metrics do not account for the sequencing of events. To do this would introduce another layer of complexity, which could be an extension of this work.

Why does precipitation occur so unevenly, and why is its change in response to warming even more uneven? Explanations for these questions can be inferred from the shape of the distribution of precipitation, its relationship to moisture and vertical velocity, and their responses to anthropogenically-forced warming (Pendergrass and Gerber, 2016). For a fixed climate state like the present, the distribution of precipitation is uneven primarily because of the nonlinear relationship between temperature and precipitation and the skewed (or asymmetric) distribution of vertical velocity. The saturation vapor pressure of water increases exponentially with temperature (according to the Clausius-Clapeyron relationship), and so the amount of water potentially available to condense varies dramatically in time at any given location. The shape of the distribution of precipitation changes in response to warming for three related reasons. First, a warmer climate has substantially more moisture because of nearly constant relative humidity and

Clausius-Clapeyron, which leads to increased precipitation; this is mitigated by increasing stability. Second, the increase in latent heat release associated with increased precipitation amplifies the circulation, increasing the unevenness of the vertical velocity distribution. Finally, to maintain energy balance despite the large increases in precipitation on the wettest days, fewer days have precipitation overall. Together, these mechanisms drive increasing unevenness of precipitation in response to climate change.

5 Conclusion

Our results show that most precipitation falls over a short period of time - half of precipitation falls in the heaviest 12 days of each year at observing stations. Climate models underestimate the unevenness in precipitation compared to station observations, but much of the difference is accounted for by resolution. The change in precipitation in response to warming is more uneven than present-day precipitation, and it occurs primarily during events often considered extreme. On the scale resolved by models (~100-200 km) in a high emissions scenario, over 80% of precipitation increase occurs beyond the 95th percentile. Twenty percent of the change occurs on the wettest 2 days each year, half on the wettest 8.6 days, and seventy percent in the wettest two weeks. At station scale, precipitation change is even more uneven: half of the change occurs on the wettest 6 days.

In contrast to temperature, where climate change can be thought of as a simple shift of the distribution, the shape of the distribution of precipitation changes with warming so that the heaviest events make up a larger fraction of total precipitation. The uneven nature of precipitation increase could exacerbate impacts like flooding and drought. Rather than assuming more rain in general, society needs to take measures to deal with little change most of the time, and a handful of events with much more rain.

Acknowledgments and Data

We thank attendees of the 2nd meeting on Monsoons and ITCZ for useful feedback. We acknowledge the WCRP's Working Group on Coupled Modelling, which is responsible for CMIP, and thank the climate modeling groups (Table S1) for producing and sharing model output (pcmdi9.llnl.gov). The U.S. Department of Energy (DOE)'s PCMDI provides coordinating support for CMIP and led development of software infrastructure in partnership with the Global Organization for Earth System Science Portals. We thank NOAA for producing and sharing GHCN-D (Menne, et al., 2012b, www1.ncdc.noaa.gov/pub/data/ghcn/daily) and NASA for TRMM 3b42 (disc.gsfc.nasa.gov). All data are available at aforementioned URLs. This research was supported by the Regional and Global Climate Modeling Program of the U.S. DOE Office of Science (BER), Cooperative Agreement DE-FC02-97ER62402.

References

Allen, M. R., and W. J. Ingram (2002), Constraints on future changes in climate and the hydrologic cycle., *Nature*, *419*(6903), 224–32, doi:10.1038/nature01092.

Chen, C. T., and T. Knutson (2008), On the verification and comparison of extreme rainfall indices from climate models, *J. Clim.*, *21*(7), 1605–1621, doi:10.1175/2007JCLI1494.1.

Collins, M. et al. (2013), Long-term climate change: Projections, commitments and irreversibility, in *Climate Change 2013: The Physical Science Basis. Contribution of Working*

Group I to the Fifth Assessment Report of the Intergovernmental Panel on Climate Change, edited by T. F. Stocker et al., pp. 1029-1136. Cambridge University Press, Cambridge, United Kingdom and New York, NY, USA, doi:10.1017/CBO9781107415324.024.

Fishman, R. (2016), More uneven distributions overturn benefits of higher precipitation for crop yields, *Environ. Res. Lett.*, *11*(2), 024004, doi:10.1088/1748-9326/11/2/024004.

Groisman, P. Y., R. W. Knight, D. R. Easterling, T. R. Karl, G. C. Hegerl, and V. N. Razuvaev (2005), Trends in intense precipitation in the climate record, *J. Clim.*, *18*(9), 1326–1350, doi:10.1175/JCLI3339.1.

Huffman, G. J., D. T. Bolvin, E. J. Nelkin, D. B. Wolff, R. F. Adler, G. Gu, Y. Hong, K. P. Bowman, and E. F. Stocker (2007), The TRMM Multisatellite Precipitation Analysis (TMPA): Quasi-Global, Multiyear, Combined-Sensor Precipitation Estimates at Fine Scales, *J. Hydrometeorol.*, *8*(1), 38–55, doi:10.1175/JHM560.1.

Karl, T. R., and R. W. Knight (1998), Secular Trends of Precipitation Amount, Frequency, and Intensity in the United States, *Bull. Am. Meteorol. Soc.*, *79*(2), 231–241, doi:10.1175/1520-0477(1998)079<0231:STOPAF>2.0.CO;2.

Konapala, G., A. Mishra, and L. R. Leung (2017), Changes in temporal variability of precipitation over land due to anthropogenic forcings, *Environ. Res. Lett.*, *12*(2), 024009, doi:10.1088/1748-9326/aa568a.

Meinshausen, M. et al. (2011), The RCP greenhouse gas concentrations and their extensions from 1765 to 2300, *Clim. Change*, *109*(1), 213–241, doi:10.1007/s10584-011-0156-z.

Menne, M. J., I. Durre, R. S. Vose, B. E. Gleason, T. G. Houston, M. J. Menne, I. Durre, R. S. Vose, B. E. Gleason, and T. G. Houston (2012a), An Overview of the Global Historical Climatology Network-Daily Database, *J. Atmos. Ocean. Technol.*, *29*(7), 897–910, doi:10.1175/JTECH-D-11-00103.1.

Menne, M.J., et al. (2012b), Global Historical Climatology Network - Daily (GHCN-Daily), Version 3.24, *NOAA Natl. Clim. Data Center.*, doi:10.7289/V5D21VHZ.

Mitchell, J. F. B., C. A. Wilson, and W. M. Cunnington (1987), On CO_2 climate sensitivity and model dependence of results, *Q. J. R. Meteorol. Soc.*, *113*(475), 293–322, doi:10.1002/qj.49711347517.

O'Neill, L. W., T. Haack, D. B. Chelton, and E. Skyllingstad (2017), The Gulf Stream Convergence Zone in the Time-Mean Winds, *J. Atmos. Sci.*, *74*(7), 2383–2412, doi:10.1175/JAS-D-16-0213.1.

Pendergrass, A. G. (2018), What precipitation is extreme?, *Science*. *360*(6393), 1072–1073, doi:10.1126/science.aat1871.

Pendergrass, A. G., and E. P. Gerber (2016), The rain is askew: Two idealized models relating vertical velocity and precipitation distributions in a warming world, *J. Clim.*, *29*(18), doi:10.1175/JCLI-D-16-0097.1.

Pendergrass, A. G., and D. L. Hartmann (2014a), Changes in the distribution of rain frequency and intensity in response to global warming, *J. Clim.*, *27*(22), doi:10.1175/JCLI-D-14-00183.1.

Pendergrass, A. G., and D. L. Hartmann (2014b), Two modes of change of the distribution of rain, *J. Clim.*, *27*(22), doi:10.1175/JCLI-D-14-00182.1.

Pfahl, S., P. A. O'Gorman, and E. M. Fischer (2017), Understanding the regional pattern of projected future changes in extreme precipitation, *Nat. Clim. Chang.*, *7*(6), 423–427, doi:10.1038/nclimate3287.

Rajah, K., T. O'Leary, A. Turner, G. Petrakis, M. Leonard, and S. Westra (2014), Changes to the temporal distribution of daily precipitation, *Geophys. Res. Lett.*, *41*(24), 8887–8894, doi:10.1002/2014GL062156.

Schär, C. et al. (2016), Percentile indices for assessing changes in heavy precipitation events, *Clim. Change*, *137*(1–2), 201–216, doi:10.1007/s10584-016-1669-2.

Semenov, V., and L. Bengtsson (2002), Secular trends in daily precipitation characteristics: Greenhouse gas simulation with a coupled AOGCM, *Clim. Dyn.*, *19*(2), 123–140, doi:10.1007/s00382-001-0218-4.

Seneviratne, S. I. et al. (2012), Changes in climate extremes and their impacts on the natural physical environment, in *Managing the Risks of Extreme Events and Disasters to Advance Climate Change Adaptation*, edited by C. B. Field et al., pp. 109–230, A Special Report of Working Groups I and II of the Intergovernmental Panel on Climate Change (IPCC). Cambridge University Press, Cambridge, United Kingdom and New York, NY, USA.

Sloat, L. L., J. S. Gerber, L. H. Samberg, W. K. Smith, M. Herrero, L. G. Ferreira, C. M. Godde, and P. C. West (2018), Increasing importance of precipitation variability on global livestock grazing lands, *Nat. Clim. Chang.*, *8*, 214-218, doi:10.1038/s41558-018-0081-5.

Stephens, G. L., T. L'Ecuyer, R. Forbes, A. Gettlemen, J. C. Golaz, A. Bodas-Salcedo, K. Suzuki, P. Gabriel, and J. Haynes (2010), Dreary state of precipitation in global models, *J. Geophys. Res. Atmos.*, *115*(24), 1–13, doi:10.1029/2010JD014532.

Sun, Y., S. Solomon, A. Dai, and R. W. Portmann (2006), How often does it rain?, *J. Clim.*, *19*(6), 916–934, doi:10.1175/JCLI3672.1.

Taylor, K. E., R. J. Stouffer, and G. A. Meehl (2012), An overview of CMIP5 and the experiment design, *Bull. Am. Meteorol. Soc.*, *93*(4), 485–498, doi:10.1175/BAMS-D-11-00094.1.

Trenberth, K. E. (1999), Conceptual framework for changes of extremes of the hydrological cycle with climate change, *Clim. Change*, *42*(1), 327–339, doi:10.1023/A:1005488920935.

Trenberth, K. E., Y. Zhang, and M. Gehne (2017), Intermittency in precipitation : duration , frequency , intensity and amounts using hourly data, *J. Hydrometeorol.*, *18*, 1393–1412, doi:10.1175/JHM-D-16-0263.1.

Zhang, X., L. Alexander, G. C. Hegerl, P. Jones, A. K. Tank, T. C. Peterson, B. Trewin, and F. W. Zwiers (2011), Indices for monitoring changes in extremes based on daily temperature and precipitation data, *Wiley Interdiscip. Rev. Clim. Chang.*, *2*(6), 851–870, doi:10.1002/wcc.147.

Figure captions

Figure 1. Unevenness of precipitation. (left) Cumulative fraction of total precipitation as a function of the number of wettest days each year, and (right) survival fraction of total precipitation as a function of percentile of all-day precipitation frequency. (a,b) Present-day observed at stations, according to TRMM 3b42 product at native 0.25° resolution and coarsened to 2.5°, and simulated by CMIP5 climate models at native resolution and regridded to 2.5°. Lines show the median across stations. Uncertainty across stations is indicated by the gray shading, which show the 25th and 75th quantiles across stations for station observations. For models, lines show the multi-model median at native and coarse resolutions. Uncertainty across models is indicated by orange envelopes, which show the range across all models at 2.5° resolution. (c,d) Simulations from CMIP5 climate models for the present, future, and change. Lines show the median across models and all land grid points. Uncertainty across models in the change is indicated by the gray envelopes, which show the range across models.

Figure 2. Unevenness of precipitation observed at stations. (a) Days per year for half of precipitation, and the fraction of annual precipitation falling on the wettest day each season: (b) DJF and (c) JJA. (d) All-day percentile for half of precipitation, and (e) fraction of precipitation occurring beyond the 95th all-day percentile. White indicates no data. Note that stations poleward of 50° are included.

442 **Table 1**

443 *Unevenness of Precipitation in Observations and Climate Models*

	Stations/grid points		Climate models, All land		
Metric	GHCN-D	Models	Present	Future (RCP8.5)	Change
1/2 of precip: percentile	97.0 percentile	94.0 percentile	93.0 percentile	93.5 percentile	98.2 percentile
1/2 of precip: days	12 wettest days	23 d	26 d	25 d	8.6 d
Fraction of precipitation					
1 day: fraction of precip	8.4 %	5.0 %	4.6 %	4.9 %	12 %
2 days	15 %	9.0 %	8.4 %	9.0 %	20 %
99^{th} percentile	26 %	16 %	15 %	16 %	39 %
5 days	30 %	18 %	17 %	18 %	39 %
14 days	55 %	38 %	34 %	36 %	67 %
95^{th} percentile	64 %	45 %	41 %	43 %	82 %
Wet day 95^{th} (> 0)	36 %	-	-	-	-
Wet day 95^{th} (≥ 1 mm/d)	24 %	-	-	-	-

444 *Note*. Median values are computed across stations or at the nearest gridpoints or over land, and
445 across models.

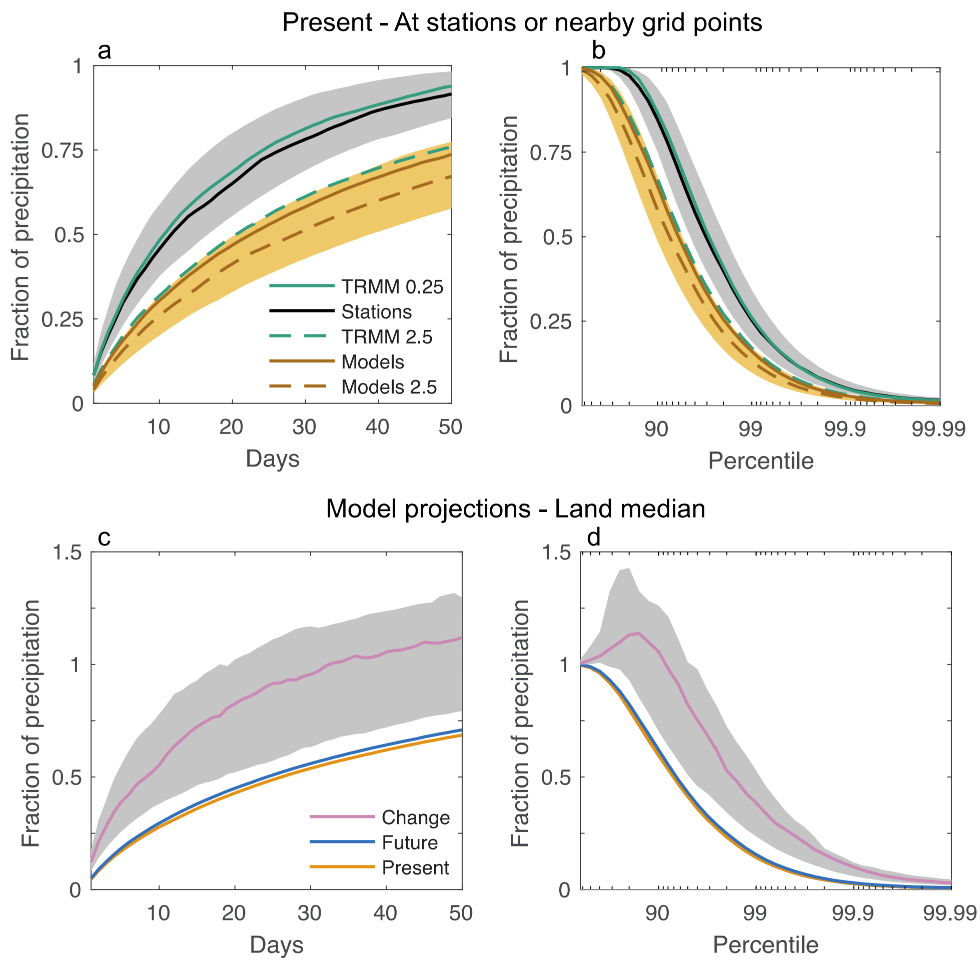

Figure 1. Unevenness of precipitation. (left) Cumulative fraction of total precipitation as a function of the number of wettest days each year, and (right) survival fraction of total precipitation as a function of percentile of all-day precipitation frequency. (a,b) Present-day observed at stations, according to TRMM 3b42 product at native 0.25° resolution and coarsened to 2.5°, and simulated by CMIP5 climate models at native resolution and regridded to 2.5°. Lines show the median across stations. Uncertainty across stations is indicated by the gray shading, which show the 25th and 75th quantiles across stations for station observations. For models, lines show the multi-model median at native and coarse resolutions. Uncertainty across models is indicated by orange envelopes, which show the range across all models at 2.5° resolution. (c,d) Simulations from CMIP5 climate models for the present, future, and change. Lines show the median across models and all land grid points. Uncertainty across models in the change is indicated by the gray envelopes, which show the range across models.

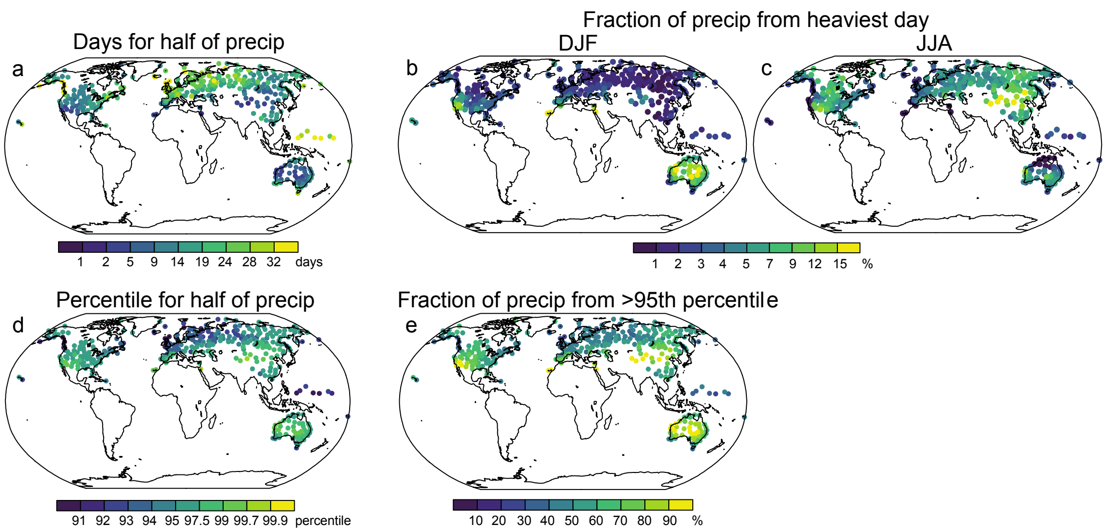

Figure 2. Unevenness of precipitation observed at stations. (a) Days per year for half of precipitation, and the fraction of annual precipitation falling on the wettest day each season: (b) DJF and (c) JJA. (d) All-day percentile for half of precipitation, and (e) fraction of precipitation occurring beyond the 95th all-day percentile. White indicates no data. Note that stations poleward of 50° are included.

Geophysical Research Letters

Supporting Information for

The uneven nature of daily precipitation and its change

Angeline G. Pendergrass[1*] and Reto Knutti[2]

[1]National Center for Atmospheric Research, Boulder, Colorado, USA

[2]Institute for Atmospheric and Climate Science, ETH-Zurich, Zurich, Switzerland

Contents of this file

Tables S1 to S3

Model	RCP 2.6	Historical and RCP 8.5	Institute
CCSM4	x	x	NCAR
CNRM-CM5	x	x	CNRM-CERFACS
CSIRO-Mk3.6.0	x	x	CSIRO-QCCCE
CanESM2	x	x	CCCMA
GFDL-CM3	x	x	NOAA GFDL
GFDL-ESM2M	x	x	NOAA GFDL
GISS-E2-H		x	NASA GISS
GISS-E2-R		x	NASA GISS
HADGEM2-CC		x	Met Office Hadley Centre
HADGEM2-ES	x	x	Met Office Hadley Centre
IPSL-CM5A-LR	x	x	IPSL
MIROC-ESM-CHEM	x	x	MIROC
MIROC-ESM	x	x	MIROC
MIROC5	x	x	MIROC
MPI-ESM-LR	x	x	MPI-M
MRI-CGCM3	x	x	MRI
NorESM1-M	x	x	NCC
BCC-CSM1-1	x	x	BCC
INMCM4		x	INM
GFDL-ESM2G	x	x	NOAA GFDL
IPSL-CM5A-MR	x	x	IPSL
FGOALS-g2	x	x	LASG-CESS
IPSL-CM5B-LR		x	IPSL
EC-EARTH		x	EC-EARTH
ACCESS1-0		x	CSIRO-BOM
ACCESS1-3		x	CSIRO-BOM
MPI-ESM-MR	x	x	MPI
CESM1(CAM5)	x	x	NSF-DOE-NCAR
CMCC-CM		x	CMCC
CESM1(BGC)		x	NSF-DOE-NCAR
HADGEM2-AO	x	x	NIMR/KMA
BNU-ESM	x	x	GCESS
BCC-CSM1.1(m)	x	x	BCC
CMCC-CMS		x	CMCC
CMCC-CESM		x	CMCC
MRI-ESM1		x	MRI

Table S1. CMIP5 models in this study.

Metric	Land	Extratropical land	Ocean	Tropics	Extratropics	Global
Present						
1/2 of precip: days	26 d	28 d	36 d	33 d	35 d	34 d
1/2 of precip: percentile	93.0 percentile	92.5 percentile	90.3 percentile	91.7 percentile	90.6 percentile	91.1 percentile
Change						
1/2 of precip: days	8.6 d	19 d	11 d	7.0 d	16 d	9.6 d
1/2 of precip: percentile	98.1 percentile	94.9 percentile	97.0 percentile	98.6 percentile	95.8 percentile	97.8 percentile
Change more uneven than present						
Fraction of models	35/36	28/36	33/36	29/36	35/36	34/36
Percent of models	97 %	78 %	92 %	81 %	97 %	94 %

Table S2. Regional breakdown of projected unevenness of precipitation and its change, in the median across models (tropical / extratropical break is at 30°), and the fraction of models where the change is more uneven than present precipitation for each region.

Metric	Present	Change: Low scenario	Change: High scenario
1/2 of precip: percentile	92.7 percentile	93.9 percentile	98.1 percentile
1/2 of precip: days	27 d	24 d	8.6 d
1 day: fraction of precip	4.5 %	7.4 %	12 %
2 days	8.1 %	14 %	21 %
99^{th} percentile	14 %	22 %	37 %
5 days	17 %	25 %	39 %
14 days	34 %	40 %	65 %
95^{th} percentile	41 %	41 %	70%

Table S3. Scenario dependence of unevenness: Comparison among the 23 models for which simulations are available from the high emissions scenario (RCP8.5) as well as a low emissions scenario (RCP2.6).